

Supporting Information

Optogenetics-inspired manipulation of synaptic memory using All-Optically Controlled memristors

Qihao Sun,^{‡,a,b,c} Zhecheng Guo,^{‡,a} Xiaojian Zhu,^{*,b,c} Qian Jiang,^{b,c,d} Huiyuan Liu,^{b,c,e} Xuerong Liu,^{b,c}
Cui Sun,^{b,c} Yuejun Zhang,^{*,a} Liu Wu,^{b,c,e} and Run-Wei Li^{b,c}

^a*Faculty of Electrical Engineering and Computer Science, Ningbo University, Ningbo 315211, P. R. China. E-mail: zhangyuejun@nbu.edu.cn*

^b*CAS Key Laboratory of Magnetic Materials and Devices, Ningbo Institute of Materials Technology and Engineering, Chinese Academy of Sciences, Ningbo 315201, P. R. China. E-mail: zhuxj@nimte.ac.cn*

^c*Zhejiang Province Key Laboratory of Magnetic Materials and Application Technology, Ningbo Institute of Materials Technology and Engineering, Chinese Academy of Sciences, Ningbo 315201, P. R. China.*

^d*College of Materials Science and Opto-Electronic Technology, University of Chinese Academy of Sciences, Beijing 100049, P. R. China.*

^e*Nano Science and Technology Institute, University of Science and Technology of China, Suzhou 215123, P. R. China.*

[‡]*These authors contributed equally to this work.*

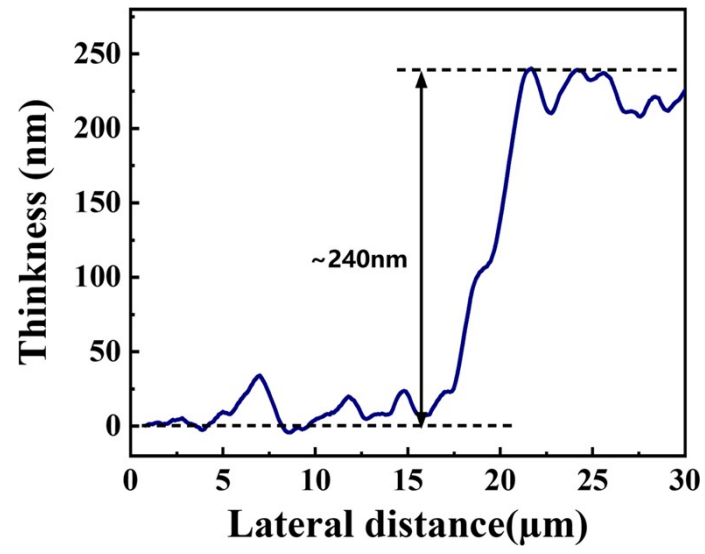


Fig. S1 The thickness of $\text{Cs}_2\text{AgBiBr}_6$ thin film.

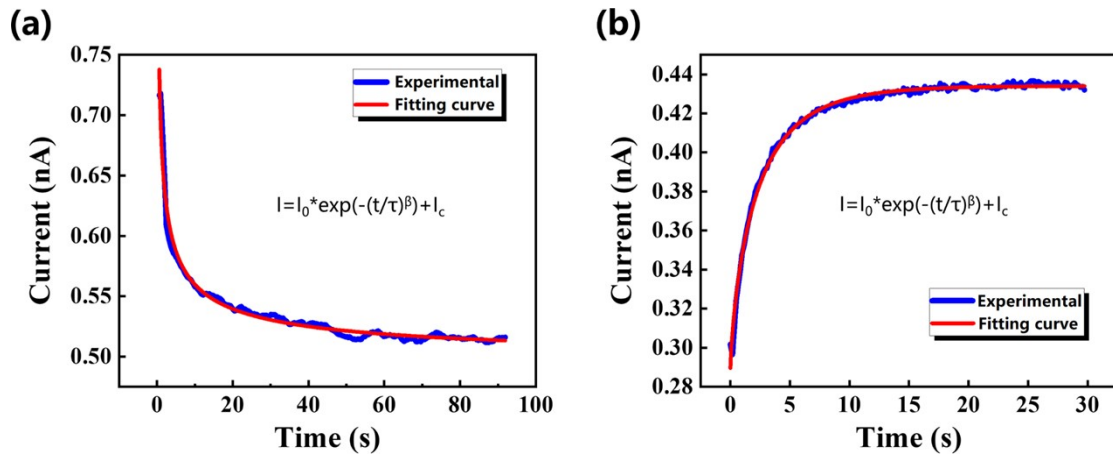


Fig. S2 Fitting result curve of current decay region in Fig. 2b (a) and Fig. 2c (b) after light was turned off.

The stretched exponential function used for fitting the attenuation region.

$$I = I_0 \cdot \exp(-(t/\tau)^\beta) + I_c \quad (1)$$

Where I_0 is a prefactor and I_c represents the background current, about 0.52nA. τ and β represent the characteristic decay time constant and the stretch index, respectively.

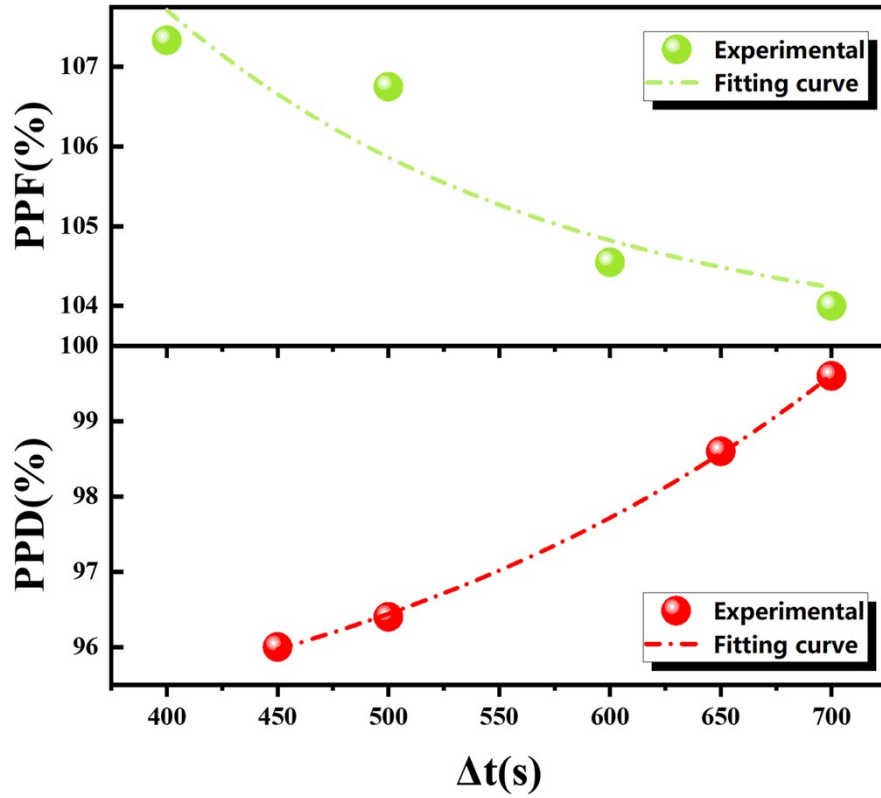


Fig. S3 The variation of PPF and PPD index with the interval of light pulse pairs (Δt).

The fitting function:

$$y = y_0 + A \cdot \exp(-\Delta t / \tau) \quad (2)$$

where A and τ are the initial facilitation magnitude and the characteristic relaxation time of the decay term, respectively.

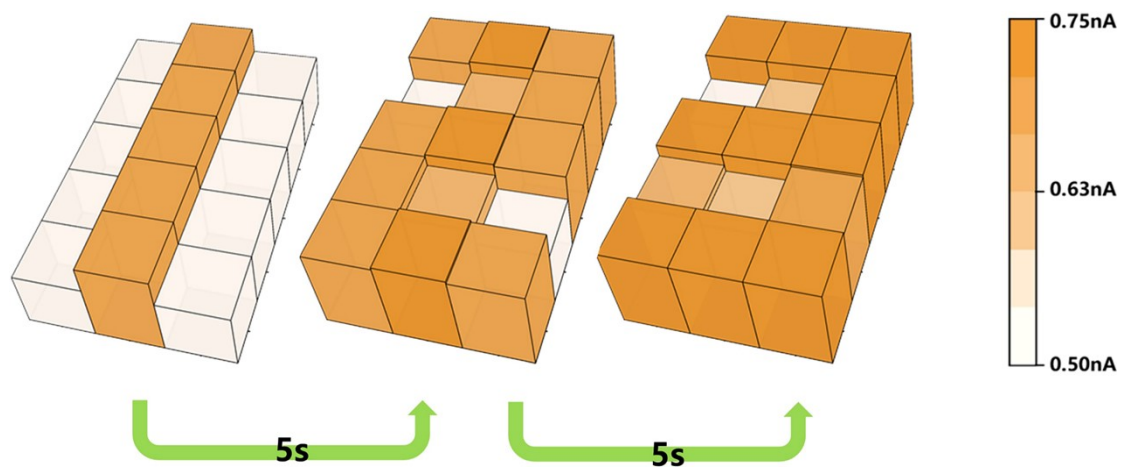
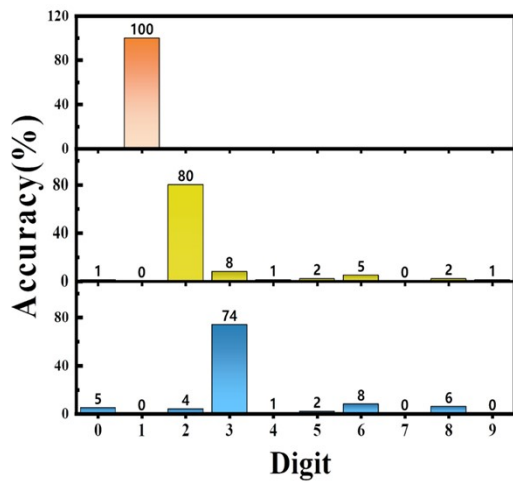


Fig. S4 Current maps measured from the array after being illuminated by green lights, showing patterns of digits “1”, “2”and “3”.

(a)



(b)

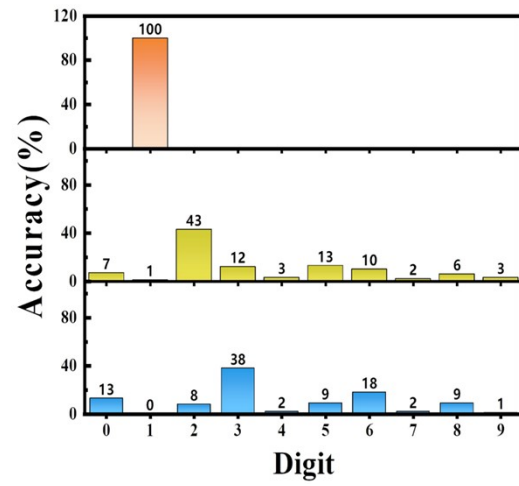


Fig. S5 The recognition accuracy of the three digits identified by the artificial neural network after the array was processed by and green-red (a) and green light (b).

Table. S1 Comparison between previously reported all-optical controlled memristors and this work.

Device structure	Mechanisms	Wavelength	Photocurrent	Ref.
Bi ₂ O ₂ Se/Graphene	The coexistence of photoconductive and bolometric effects; light-induced physical gas desorption and adsorption.	365nm; 635nm	~1-10μA	1
Ni/MAPbBr ₃ -ZnO/Ni	The increase and diffusion of photogenerated charge carriers.	365nm; 520nm	~0.1-10μA	2
Pyr-GDY/Gr/PbS	The strong photogating effect induced by Pyr-GDY and PbS QDs.	450nm; 980nm	~1-10μA	3
Au/Black Phosphorus/Au	The electron-hole pair generation after UV absorption; Oxygen adsorption on BP surface.	280nm; 365nm	~1-10μA	4
Au/Cs ₂ AgBiBr ₆ /Au	The electron detrapping and trapping in the defects.	405nm; 532nm; 660nm	<1nA	This work

References:

1. C. M. Yang, T. C. Chen, D. Verma, L. J. Li, B. Liu, W. H. Chang and C. S. Lai, *Adv. Funct. Mater.*, 2020, **30**, 2001598.
2. S. Ge, F. Huang, J. He, Z. Xu, Z. Sun, X. Han, C. Wang, L. B. Huang and C. Pan, *Adv. Optical Mater.*, 2022, **10**, 2200409.
3. Y. X. Hou, Y. Li, Z. C. Zhang, J. Q. Li, D. H. Qi, X. D. Chen, J. J. Wang, B. W. Yao, M. X. Yu, T. B. Lu and J. Zhang, *ACS Nano*, 2021, **15**, 1497-1508.
4. T. Ahmed, S. Kuriakose, E. L. H. Mayes, R. Ramanathan, V. Bansal, M. Bhaskaran, S. Sriram and S. Walia, *Small*, 2019, **15**, e1900966.